

Igneous Rock Classification At Gale (Sols 13-800). A. Cousin¹, V. Sautter², N. Mangold³, C. Fabre⁴, O. Forni⁵, W. Rapin⁵, M. Fisk⁶, O. Gasnault⁵, N. Lanza¹, J. Lasue⁵, P.-Y. Meslin⁵, H. Newson⁷, A. Ollila⁸, V. Payre⁴, R.C. Wiens¹, S. Maurice⁵, and ChemCam Team. ¹LANL, Los Alamos, USA; ²MNHN, Paris, France; ³LPGN, Nantes, France; ⁴G2E, Nancy, France; ⁵IRAP, Toulouse, France; ⁶College of Earth, Ocean, and Atmospheric Sciences, OR, USA; ⁷UNM, Albuquerque, USA; ⁸Chevron, Houston, TX, USA [agnescousin@icloud.com]

Introduction: Textural and compositional analyses using MastCam [1] and ChemCam [2,3] instruments have identified a total of 53 massive (non layered) igneous targets. These range from mafic targets where feldspars form less than 50% of the rock to felsic samples where feldspars are the dominant mineral. These rocks have been described as floats on Bradbury Rise [4] and all along the traverse up to sol 800. This work presents a classification of these 53 igneous targets. A companion abstract [5] focuses in more detail on ten of the most feldspar-rich and alkaline targets.

Methodology: Textures have been assessed using images. MastCam and RMI cameras allow the distinction of grain shape distribution. The smallest visible grain seen by RMI corresponds to 95 μm at 2.4m or 140 μm at 3.6 m. MastCam is particularly useful also to provide color images and context.

ChemCam's LIBS analysis uses a 300-500 μm analysis footprint to sample the targets over multiple locations (11520 spectra taken on > 384 points for these 53 targets). Independent component analyses (ICA) is used to assess lateral heterogeneity between different points within a raster on a given rock target, as well as chemical variation with depth within a shot sequence [6]. Quantification of key element ratios from the spectral characteristics of the target is performed by univariate analysis [7] which derives quantitative estimates from peak areas of well-chosen LIBS lines using on board calibration targets (CCCTs) [8]. ChemCam offers thus the first opportunity to assess mineralogical diversity at grain-size scales and, from this, lithological diversity.

Rock morphology and texture: The rocks are mainly floats or form clasts in conglomerates (Fig.1). They are heterogeneous, grade in color from dark gray to light-toned with many faceted rocks due to wind erosion.

From their morphology and texture, five groups have been clearly identified [9] and are listed in Table 1: (1) dark aphanitic/phaneritic rocks with few light-toned microliths. Some of them are shiny with no visible grains and with conchoidal fractures (21 rocks - Fig. 1a), (2) porphyritic rocks with light-toned euhedral phenocrysts (up to 20 mm in length) set in a dark mesostasis (9 rocks - Fig. 1b), (3) leucocrate rocks with no visible grains, sometimes vesiculated or forming slabs covered by dust (6 rocks - Fig. 1c), (4) dark rocks either fine (< 1mm) or coarse grained (> 1mm) with same amount of dark and light equigranular crystals (8 rocks - Fig. 1d), (5) leucocrate coarse grained

(> 4mm) rocks either pristine or chunky; the later won't be used for their chemistry (9 rocks - Fig. 1e).

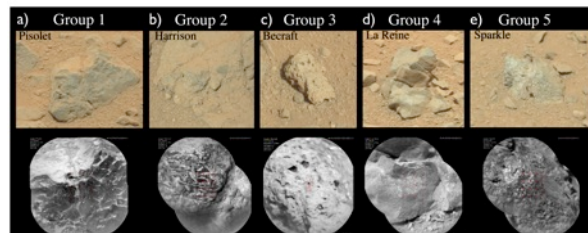


Figure 1: Rock morphology from MastCam and RMI images, for each emblematic target/group. A) Group 1, Pisolet (sol 332), B) Group 2, Harrison (sol 512), C) Group 3, Becraft (sol 421), D) Group 4, La Reine (sol 346) and E) Group 5, Sparkle (sol 514).

Group 1		Group 2		Group 4		Group 5	
Sol	Target	Sol	Target	Sol	Target	Sol	Target
329	Gunflint	19	Peacock Hill	13	Coronation	511	Clinton
329	Watterson	365	Robin Hood	192	Mara	514	Sparkle
332	Pisolet	379	Stoek	346	La Reine	356	Norris 2
367	Black Head	390	Falla	337	Ashuaampi	544	Nita
370	Fleur de Lys	407	Horlick	376	Beacon		
377	Aztec	512	Harrison	349	Black Trout	358	Bird River
465	Tully	544	Bindi	557	King Leopold	358	Little Wind River
691	Limekiln	553	Angelo	646	Exceter	365	Wilkinson
692	Pyramidal Hills	654	Albee			379	Ross
694	South Park 2					522	Dougalls
694	Johmie						
700	Chocolate Sunday Mountain						
700	Skidoo						
704	Thimble						
713	Thornike						
730	CC BT 0730	13	Blanchet				
731	Eagle Mountain	19	Stark				
732	Keeler Canyon	338	Chakoinau				
733	Furnace Creek	379	Sledger				
733	Red Pass	421	Becraft				
739	Warm Spring	653	Meeting House				

Table 1: List of igneous targets used for this study, ranked by sol number and grouped by morphology and texture analysis.

From textural analyses it is possible to distinguish 36 rocks with effusive texture ranging from glassy to porphyritic (groups 1, 2, 3), and 17 intrusive rocks ranging from aphanitic/phaneritic to porphyritic (groups 4 & 5). From the images, the ratio of light-toned minerals to dark-toned minerals allows further identification of mafic and felsic sub-groups within effusive and intrusive classes. Note that vesiculated rocks of group 3 could be either pumice or melted rocks resulting from impact.

For this study, we have voluntarily omitted 18 targets which are interpreted to be igneous but classified as "uncertain texture", as Jake-M target [10].

Chemical composition and mineral inference The 53 anhydrous targets have been plotted by molar Al/Si vs. (Fe+Mg)/Si (Fig. 2a) where felsic minerals (quartz, plagioclase solid-solution, nepheline) plot on the Y-axis whilst mafic ones (HCP, LCP, olivine, oxides) plot on the X-axis. Rocks in group 3 plot on or close to the Y-axis in figure 2a. Light-toned intrusive rocks (group 5, in red) such as Sparkle plot on a mixing line between oligoclase-albite (Al/Si: 0.48-0.33 ; An30-0)

and a silica-rich component. Vesiculated light-toned rocks such as Becraft (group 3, in brown) have compositions close to the macusanite CCCT, a rhyolitic glass ($Al/Si < 0.33$), indicative of silica saturated rocks mixed with an alkali-feldspar component. Porphyritic effusive targets (group 2) and coarse-grained intrusives (group 4, in green) plot on the same mixing line between oligoclase ($Al/Si = 0.38-0.44$; $An = 10-28$) and mafic compositions. Just one rock, Mara (group 4), plots on a noritic trend joining andesine and pigeonite. Rocks from group 1 with barely visible grains plot (in blue) in the middle of the basaltic mixing line within the blue ellipse.

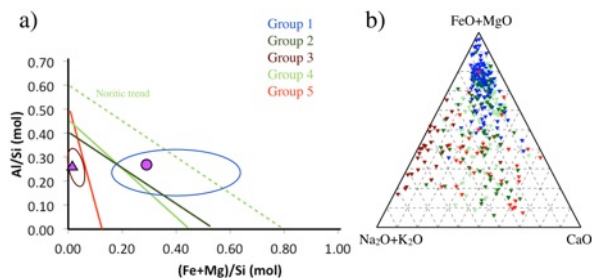


Figure 2: a) Al/Si vs. $(Fe+Mg)/Si$ (molar ratios) diagram. Only trends are shown for each group for clarity. b) FM-C-NK ternary diagram. These quantitative values have been retrieved using the univariate technique. The pink triangle and circle correspond to macusanite and shergottite CCCTs.

Group 5 felsic rocks show an enrichment in Ca and Si whereas group 3 felsic rocks plot closer to the alkali endmember (Fig. 2b). Figure 2 (a and b) shows that group 5 felsic rocks are plagioclase rich whereas group 3 felsic rocks are enriched in alkali feldspars.

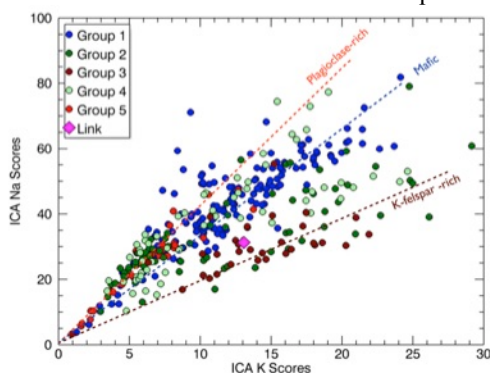


Figure 3: ICA Na vs. K ICA scores (coefficient correlations) showing a clear distinction between the two felsic groups (3 and 5, in brown and red, resp.).

This distinction can also be observed in Fig. 3 where the group 3 felsic rocks (in brown) plot close to Link, which was one of the first K-rich conglomerate targets observed with ChemCam [11], whereas felsic group 5 shows a higher Na/K ratio (in red). Some of the porphyritic points (in dark green) plot close to the group 3 alkali-rich targets. Those points correspond to some k-rich zoning of plagioclase phenocrysts ob-

served on these porphyritic targets, such as Harrison [12]. Moreover, group 3 felsic targets show a higher Ba content and Rb signal than in any other groups, suggesting the existence of K-rich feldspars [13].

Whole rocks estimation for each group Tentative whole rocks calculation were computed when possible. For the intrusive rocks (group 4 & 5), only targets with at least 9 points analysis are taken into account: an average of all points should be able to give access to the whole rock composition. For targets with aphanitic textures (group 1 & 3), minerals are smaller to the laser beam; therefore an average of all locations for each rock gives a good estimation. In group 2, only Harrison's composition has been constrained through a combination of modal proportions and average composition of felsic and mafic phases [12].

The whole-rock composition allows us to distinguish two trends: a quartz-normative trend including rocks from group 5 which are close to diorite/granodiorite; groups 2 and 3 are nepheline-normative and plot in the trachyandesite field (group 2) and trachyte field (group 3). Group 1 plots between basanite and basalt [See [5] for more details].

Conclusion This study focuses on igneous targets starting from their textures based on images but clearly corroborated by the compositional data. These igneous rocks revealed a large variability, from intrusive to effusive, with basaltic up to felsic compositions (plagioclase or alkali-feldspars – rich rocks). Group 3 rocks contain exclusively Si, Al, Na and K as major element and high Ba content; they are the first felsic alkali-rich volcanic rocks analyzed in situ so far on Mars. Some of their texture suggest that they could be impact melt.

Chemical variations exist inside each group suggesting that groups based on texture do not imply a unique composition, but overall there is a good consistency between texture and chemistry that allow a first-order interpretation for these groups. So we propose that Group 1 would correspond to basalt/basanite rocks and Group 2 to trachyandesite targets; Trachytes would belong to Group 3; Group 4 would correspond to gabbro/norites, and Group 5 to granodiorites/diorites rocks. Gale is often described as a sedimentary terrain; the presence and variability of igneous rocks, as detected by CCAM from sol 13, should not be underestimated. Moreover, such a variety of igneous rocks has important implications for the globally averaged Mars compositions and for the formation of the southern highlands.

References: [1] Bell III et al. 2012, LPSC #2541, [2] Wiens et al. 2012, Space Science Reviews 170, [3] Maurice et al. 2012, Space Science Reviews 170, [4] Sautter et al. 2014, JGR-Planets, [5] Sautter et al., this meeting, [6] Forni et al. 2013, SAB, [7] Fabre et al. 2014, SAB, [8] Fabre et al. 2011, SAB, [9] Sautter et al. 2014, #1369 LPSC 2014, [10] Stolper et al. 2013, Science 341, [11] Mangold et al. 2013 LPSC #1267, [12] Sautter et al. 2014, Mars 8th conference, [13] Ollila et al. 2013 JGR-Planets.